2200 *Inorg. Chem.* **1989**, *28*, 2200-2204

Contribution from the Department of Chemistry,
The University of North Carolina at Chapel Hill, Chapel Hill, North Carolina 27514

Electronic Structure of the Oxidation Catalyst *cis*-$[Ru^{IV}(bpy)_2(py)(O)](ClO_4)_2$

John C. Dobson, Jeffrey H. Helms, Pascal Doppelt, B. Patrick Sullivan, William E. Hatfield,* and Thomas J. Meyer*

Received January 9, 1989

The temperature variation of the magnetic susceptibility of *cis*-$[Ru^{IV}(bpy)_2(py)(O)](ClO_4)_2$ (bpy is 2,2′-bipyridine and py is pyridine) has been determined in the solid state and in CD_3CN by ^1H NMR measurements. The complex possesses a nonmagnetic ground state with the first excited state lying 79 cm^{-1} higher in energy in the solid state and 56 cm^{-1} in solution. The implications of spin character for the oxidative 2e atom-transfer reactivity of the ion are discussed.

Introduction

A series of polypyridyl complexes of Ru are known that contain aqua ligands.[1] A notable feature in their chemistry is the appearance of a series of oxidation states that are accessible over a relatively narrow range in redox potentials, e.g., eq 1.[1a,b] Access

$$\textit{cis}\text{-}[Ru^{II}(bpy)_2(py)(OH_2)_2]^{2+} \underset{+e^-,\ +H^+}{\overset{-e^-,\ -H^+}{\rightleftharpoons}} \textit{cis}\text{-}[Ru^{III}(bpy)_2(py)(OH)]^{2+} \underset{+e^-,\ +H^+}{\overset{-e^-,\ -H^+}{\rightleftharpoons}} \textit{cis}\text{-}[Ru^{IV}(bpy)_2(py)(O)]^{2+} \quad (1)$$

to the higher oxidation states relies on proton loss and the electronic stabilization provided by Ru^{IV}–oxo formation. Crystal structures of complexes containing the $Ru^{IV}{=}O$ group show considerable Ru–O multiple-bond character arising from O → Ru(IV) donation.[2]

The high-oxidation-state oxo complexes of Ru are efficient stoichiometric and/or catalytic oxidants in a series of organic and inorganic oxidations.[3,4] An important part of that chemistry has been the extensive mechanistic and catalytic properties that have been uncovered for *cis*-$[Ru^{IV}(bpy)_2(py)(O)]^{2+}$ and related complexes. Well-defined oxidative pathways have been identified for this oxidant that involve H atom or hydride transfer to the Ru^{IV}–oxo group (b is 2,2′-bipyridine)[5,6]

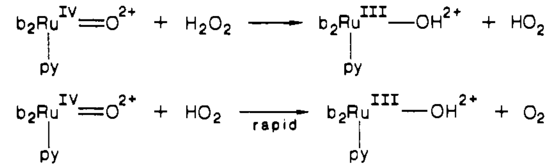

$$b_2(py)Ru^{IV}{=}O^{2+} + H_2O_2 \longrightarrow b_2(py)Ru^{III}{-}OH^{2+} + HO_2 \quad (2)$$
$$b_2(py)Ru^{IV}{=}O^{2+} + HO_2 \xrightarrow[\text{rapid}]{} b_2(py)Ru^{III}{-}OH^{2+} + O_2$$

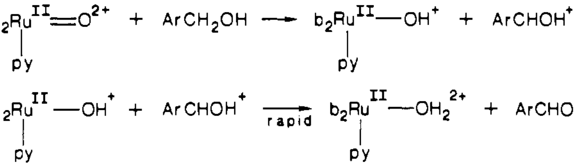

$$b_2(py)Ru^{II}{=}O^{2+} + ArCH_2OH \longrightarrow b_2(py)Ru^{II}{-}OH^{+} + ArCHOH^{+} \quad (3)$$
$$b_2(py)Ru^{II}{-}OH^{+} + ArCHOH^{+} \xrightarrow[\text{rapid}]{} b_2(py)Ru^{II}{-}OH_2^{2+} + ArCHO$$

or O atom transfer from the Ru^{IV}–oxo group[7] (S is solvent)

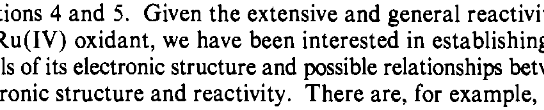

$$b_2(py)Ru^{IV}{=}O^{2+} + PPh_3 \longrightarrow b_2(py)Ru^{II}{-}O{=}PPh_3^{2+} \quad (4)$$

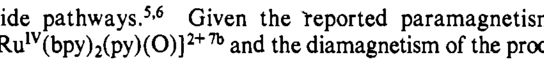

$$b_2(py)Ru^{IV}{=}O^{2+} + ArNO \xrightarrow{S} b_2(py)Ru^{II}{-}S^{2+} + ArNO_2 \quad (5)$$

In the d^4 Ru(IV) oxidants the Ru^{IV}–oxo group imparts some special reactivity characteristics. The electron-acceptor capability of the oxidant lies in the vacancies in the dπ orbitals. The O atom of the oxo group acts as a "lead in" atom in the initial electronic interaction with the substrate. It also acts as a proton binding site following H atom or hydride transfer (reactions 2 and 3) or as a source of O^{2-} following electron transfer to the metal as in reactions 4 and 5. Given the extensive and general reactivity of the Ru(IV) oxidant, we have been interested in establishing the details of its electronic structure and possible relationships between electronic structure and reactivity. There are, for example, such reactivity features as the remarkably high k_H/k_D kinetic isotope effects that have been observed for this oxidant in H atom or hydride pathways.[5,6] Given the reported paramagnetism of *cis*-$[Ru^{IV}(bpy)_2(py)(O)]^{2+}$[7b] and the diamagnetism of the products of reactions 3–5, the possibility also exists that spin effects could play an important role in the reactivity of the oxidant.

Experimental Section

Reagents and Solvents. $RuCl_3{\cdot}3H_2O$, 2,2′-bipyridine, and all NMR grade deuterated solvents were purchased from Aldrich Chemical Co. All other materials were reagent grade and were used without further purification.

Preparations. The syntheses of *cis*-$[Ru(bpy)_2Cl_2]{\cdot}2H_2O$,[8] *cis*-$[Ru(bpy)_2(py)Cl](PF_6)$,[1b] and *cis*-$[Ru(bpy)_2(py)(O)](ClO_4)_2$[1b] have been described previously. *Caution!* Although the preparations of the perchlorate salts described here have been reported numerous times without incident, perchlorate salts of organometallic cations, metal complexes, or organic cations have been known to explode spontaneously. Therefore, the preparation and handling of the perchlorate salts deserve particular care.

***cis*-$[Ru^{II}(bpy)_2(py)(OH_2)](ClO_4)_2$.** The previously reported preparation[1b] of this salt was modified as follows: To 50 mL of 2:1 acetone–water was added 0.4 g (0.554 mmol) of $[Ru(bpy)_2(py)Cl](PF_6)$ and 0.231 g (1.18 mmol) of $AgClO_4$. The solution was heated at reflux for 75 min and allowed to cool to room temperature. The solution was filtered through a fine glass frit and the filtrate reduced in volume to -18 mL on a rotary evaporator. To the remaining solution was added 1 mL of saturated $NaClO_4(aq)$. The solution was placed in a refrigerator for $^1/_2$ h, after which time the precipitate was collected by filtration onto a medium glass frit. The precipitate was washed with 3 × 1 mL portions of cold distilled water followed by 3 × 1 mL portions of anhydrous diethyl ether and dried in vacuo; yield 0.323 g, 77%.

---

(1) (a) Moyer, B. A.; Meyer, T. J. *J. Am. Chem. Soc.* **1978**, *100*, 3601. (b) Moyer, B. A.; Meyer, T. J. *Inorg. Chem.* **1981**, *20*, 436. (c) Gersten, S. W.; Samuels, G. J.; Meyer, T. J. *J. Am. Chem. Soc.* **1982**, *104*, 4029. (d) Takeuchi, K. J.; Samuels, G. J.; Gersten, S. W.; Gilbert, J. A.; Meyer, T. J. *Inorg. Chem.* **1983**, *22*, 1407. (e) Takeuchi, K. J.; Thompson, M. S.; Pipes, D. W.; Meyer, T. J. *Inorg. Chem.* **1984**, *23*, 1845. (f) Honda, K.; Frank, A. J. *J. Chem. Soc., Chem. Commun.* **1984**, 1635. (g) Gilbert, J. A.; Eggleston, D. S.; Murphy, W. R.; Geselowitz, D. A.; Gersten, S. A.; Hodgson, D. J.; Meyer, T. J. *J. Am. Chem. Soc.* **1985**, *107*, 3855. (h) Collin, J. P.; Sauvage, J. P. *Inorg. Chem.* **1986**, *22*, 1407. (i) Marmion, M. E.; Takeuchi, K. J. *J. Am. Chem. Soc.* **1986**, *108*, 510. (j) Che, C. M.; Wong, K. Y.; Leung, W. H.; Poon, C. K. *Inorg. Chem.* **1986**, *25*, 345. (k) Che, C. M.; Tang, T. W.; Poon, C. K. *J. Chem. Soc., Chem. Commun.* **1984**, 641.

(2) (a) Yukawa, Y.; Aoyagui, K.; Kurihara, M.; Shirai, K.; Shimizu, K.; Mukaida, M.; Takeuchi, T.; Kakihana, H. *Chem. Lett.* **1985**, 283. (b) Che, C. M.; Wong, K. Y.; Mak, T. C. M. *J. Chem. Soc., Chem. Commun.* **1985**, 546.

(3) (a) Green, G.; Griffith, W. P.; Hollingshead, D. M.; Ley, L. V.; Schroder, M. *J. Chem. Soc., Perkin Trans. 1* **1984**, 681. (b) Gulliver, D. J.; Levason, W. *Coord. Chem. Rev.* **1982**, *46*, 1.

(4) (a) Meyer, T. J. *J. Electrochem. Soc.* **1984**, *131*, 221c. (b) Thompson, M. S.; Degiovani, W. F.; Moyer, B. A.; Meyer, T. J. *J. Org. Chem.* **1984**, *49*, 4972.

(5) (a) Gilbert, J. A.; Roecker, L.; Meyer, T. J. *Inorg. Chem.* **1987**, *26*, 1126. (b) Binstead, R. A.; Meyer, T. J. *J. Am. Chem. Soc.* **1987**, *109*, 3287.

(6) (a) Roecker, L.; Meyer, T. J. *J. Am. Chem. Soc.* **1987**, *109*, 746. (b) Roecker, L.; Meyer, T. J. *J. Am. Chem. Soc.* **1986**, *108*, 4066.

(7) (a) Seok, W. K.; Meyer, T. J. Manuscript in preparation. (b) Moyer, B. A.; Sipe, B. K.; Meyer, T. J. *Inorg. Chem.* **1981**, *20*, 1475. (c) Roecker, L.; Dobson, J. C.; Meyer, T. J. *Inorg. Chem.* **1987**, *26*, 779.

(8) (a) Sullivan, B. P.; Salmon, D. J.; Meyer, T. J. *Inorg. Chem.* **1978**, *12*, 3334. (b) Lay, P. A.; Sargeson, A. M.; Taube, H. *Inorg. Synth.* **1986**, *24*, 291.

0020-1669/89/1328-2200$01.50/0 © 1989 American Chemical Society

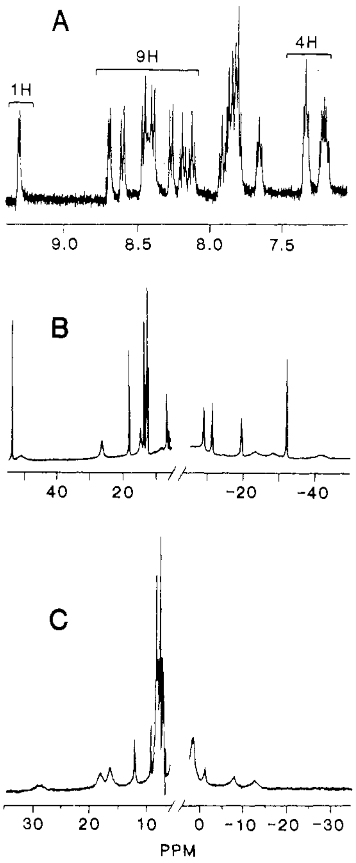

Figure 1. ^1H NMR spectra: (A) *cis*-$[Ru^{II}(bpy)_2(py)(OH_2)](ClO_4)_2$ in D_2O vs DSS; (B) *cis*-$[Ru^{IV}(bpy)_2(py)(O)](ClO_4)_2$ in CD_3CN vs TMS; (C) *cis*-$[Ru^{III}(bpy)_2(py)(OH)](ClO_4)_2$ in D_2O vs DSS.

$[Ru^{II}(bpy)_2(py\text{-}d_5)(OH_2)](ClO_4)_2$ and $[Ru^{IV}(bpy)_2(py\text{-}d_5)(O)](ClO_4)_2$. The perdeuterated pyridyl complexes were prepared by using the previously reported synthesis for the protio analogues.

NMR. All Fourier transform ^1H NMR measurements were performed on either an IBM AC200 200-MHz spectrometer or a Varian VXR400 400-MHz spectrometer. Variable-temperature studies were carried out on the latter with a Varian variable-temperature accessory calibrated with methanol by the Van Geet method.[9] For paramagnetic spectra a sweep width of 200 ppm and an acquisition time of 0.2 s were typical. Chemical shift values were referenced to tetramethylsilane (TMS) for spectra recorded in CD_3CN and to sodium 4,4-dimethyl-4-silapentane-1-sulfonate (DSS) for spectra recorded in D_2O.

Magnetic Susceptibility. Magnetic susceptibility data, in the temperature range 77–300 K, were collected on a polycrystalline sample weighing approximately 20 mg by using a computer-controlled Faraday balance. The balance consisted of a Cahn 2000 electrobalance and an ANAC 4-in. electromagnet equipped with Lewis coils[10] and a bipolar current-regulated power supply from George Associates, Berkeley, CA. A Tektronix 4052A computer and a Hewlett-Packard 3495A scanner with a relay actuator were used for automated data collection. Samples were contained in a closed glass system, which was evacuated and filled with helium gas before measurements were made. Variable temperatures were obtained by surrounding the sample zone with a Dewar flask containing liquid nitrogen. The liquid nitrogen was allowed to evaporate, and the temperature of the system increased gradually as the level of the liquid decreased in the Dewar. A single set of measurements required approximately 10 h. Sample temperatures were measured with a calibrated gallium arsenide diode and a Fluke 8502A 6.5-place voltmeter. The balance was calibrated with mercury tetrakis(thiocyanato)cobaltate(II).[11-13] The diode was placed in the sample zone within 2–3 mm of the sample bucket.

In the temperature range 4.2–80 K, magnetic susceptibility measurements were collected with the use of a Foner type[14] Princeton Applied Research Model 155 vibrating-sample magnetometer (VSM) at 10 kOe. The VSM magnet (Magnion H-96), power supply (Magnion HSR-1365), and associated field control unit (Magnion FFC-4 with a Rawson-Lush Model 920 MCM rotating-coil gauss meter) were calibrated by using procedures described earlier.[15] The VSM was calibrated with mercury tetrakis(thiocyanato)cobaltate(II),[11-13] and temperatures were measured with a gallium arsenide diode that had been standardized against a commercially calibrated diode.[16] Powdered samples (approximately 150 mg) of the calibrant and compound used in this study were contained in precision-milled Lucite sample holders. The data collected on the VSM and Faraday balance were corrected for the diamagnetism of the constituent atoms by using Pascal's constants.[17-19]

Table I. Chemical Shifts of the Bipyridyl 6′-Proton Nearest to the Ligand L in Complexes of the Type $[Ru^{II}(bpy)_2(py)(L)]^{n+}$ in CD_3CN vs TMS

salt	δ(6′-H), ppm
$[Ru^{II}(bpy)_2(py)_2]Cl_2$	8.89
$[Ru^{II}(bpy)_2(py)(OH_2)](ClO_4)_2$	9.20
$[Ru^{II}(bpy)_2(py)(OS(CH_3)_2)](ClO_4)_2$	9.28
$[Ru^{II}(bpy)_2(py)(NO)](PF_6)_3$	9.31
$[Ru^{II}(bpy)_2(py)(NCCH_3)](ClO_4)_2$	9.42
$[Ru^{II}(bpy)_2(py)(NO_2)](PF_6)$	9.88
$[Ru^{II}(bpy)_2(py)Cl](PF_6)$	9.95
$[Ru^{II}(bpy)_2(py)Br](PF_6)$	10.12
$[Ru^{II}(bpy)_2(py)(S(O)(CH_3)_2)](ClO_4)_2$	10.23

Results

^1H NMR Spectra. The ^1H NMR spectrum of *cis*-$[Ru^{II}(bpy)_2(py)(OH_2)]^{2+}$ in D_2O is shown in Figure 1A. In the spectrum 16 nonequivalent proton resonances appear for the cis 2,2′-bipyridyl ring protons as well as resonances for the 5 pyridyl protons. This is the expected pattern for C_s symmetry. Resonances in the multiplets centered at 8.41 and 7.81 ppm as well as the triplet centered at 7.32 ppm were assigned to the 2,6-H, 4-H, and 3,5-H pyridyl protons by comparison with the spectrum of *cis*-$[Ru^{II}(bpy)_2(py\text{-}d_5)(OH_2)]^{2+}$. The isolated doublet at high field can be assigned to the bipyridyl 6′-proton nearest to the OH_2 ligand on the basis of previous assignments.[7c,20]

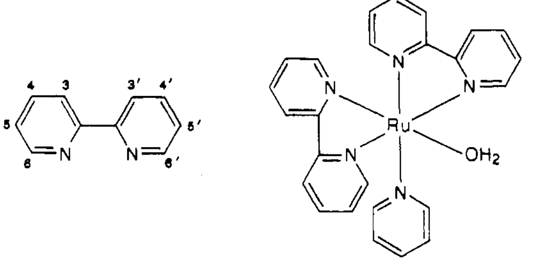

The primed notation refers to those two pyridyl rings of the bipyridyl ligands that are trans to one another. Molecular models show that the 6′-proton of the bipyridyl ligand whose adjacent ring is trans to the pyridyl ligand lies in the ring current of the pyridyl ligand and is shifted upfield. In complexes of the type *cis*-$[Ru^{II}(bpy)_2(py)(L)]^{n+}$ the chemical shift of this 6′-proton is sensitive to both the nature of L and, to a lesser extent, the solvent. The chemical shift values for the magnetically distinct 6′-H nearest to the ligand L for a series of complexes of this type are summarized in Table I.

Oxidation of *cis*-$[Ru^{II}(bpy)_2(py)(OH_2)]^{2+}$ by two electrons with concomitant loss of two protons results in formation of the paramagnetic Ru(IV) $(d\pi)^4$ oxo complex *cis*-$[Ru^{IV}(bpy)_2(py)$-

---

(9) Van Geet, A. L. *Anal. Chem.* **1968**, *40*, 2227.
(10) Lewis, R. T. *Rev. Sci. Instrum.* **1971**, *42*, 31.
(11) Figgis, B. N.; Nyholm, R. S. *J. Chem. Soc.* **1959**, 4190.
(12) Brown, D. B.; Crawford, V. H.; Hall, J. W.; Hatfield, W. E. *J. Phys. Chem.* **1977**, *81*, 1303.
(13) St. Rade, H. *J. Phys. Chem.* **1973**, *77*, 424.
(14) Foner, S. *Rev. Sci. Instrum.* **1959**, *30*, 548.
(15) Hatfield, W. E.; Losee, D. B. *Phys. Rev. B* **1974**, *10*, 212.
(16) Type TG-100 FPA (Special), No. 4277, Lake Shore Cryotronics, Westerville, OH.
(17) Figgis, B. N.; Lewis, J. In *Modern Coordination Chemistry*; Lewis, J., Wilkins, R. G., Eds.; Interscience: New York, 1960; Chapter 6, p 403.
(18) Konig, E. *Magnetic Properties of Transition Metal Compounds*; Springer-Verlag: New York, 1966.
(19) Weller, R. R.; Hatfield, W. E. *J. Chem. Educ.* **1979**, *56*, 652.
(20) Constable, E. C.; Seddon, K. R. *J. Chem. Soc., Chem. Commun.* **1982**, 34.

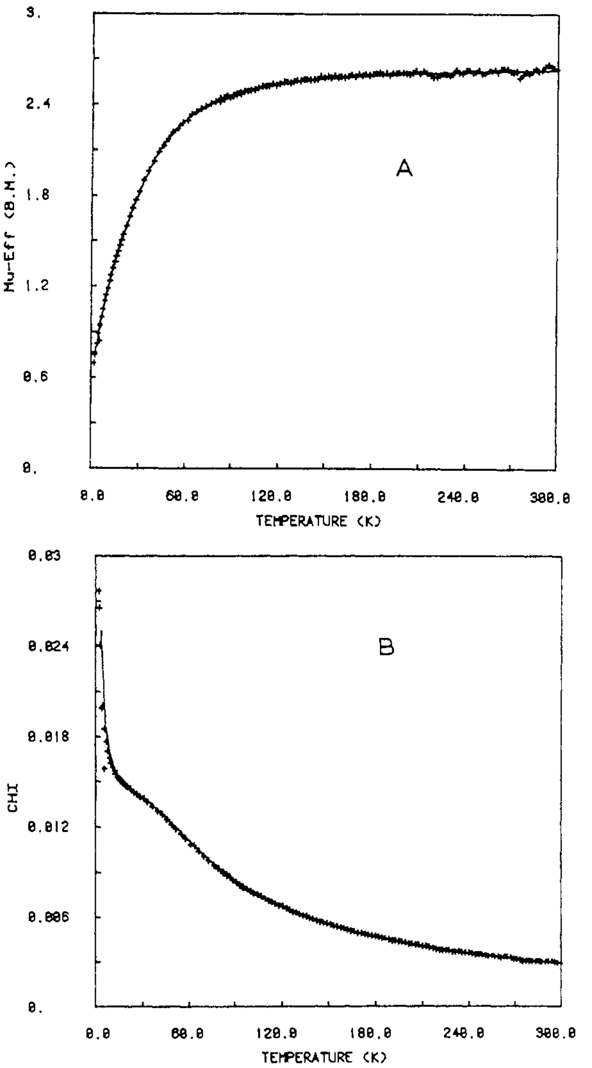

Figure 2. (A) Variable-temperature magnetic moment data for *cis*-$[Ru^{IV}(bpy)_2(py)(O)](ClO_4)_2$. (B) Variable-temperature magnetic susceptibility data for *cis*-$[Ru^{IV}(bpy)_2(py)(O)](ClO_4)_2$.

$(O)]^{2+}$. The previously reported room-temperature magnetic moment of $\mu_{eff} = 2.94\ \mu_B$ for the Ru(IV) oxo complex is close to the expected spin-only value for two unpaired electrons ($2.83\ \mu_B$).[1b] The origin of the paramagnetism in the $(d\pi)^4$ $Ru^{IV}{=}O^{2+}$ ion arises from the electronic asymmetry in $d\pi$ levels. The effect of the paramagnetism on the ^1H NMR spectrum of this complex is shown in Figure 1B. By a comparison of the spectrum of this complex with that of its deuterio analogue *cis*-$[Ru^{IV}(bpy)_2(py\text{-}d_5)(O)]^{2+}$, the broad resonance at 51.30 ppm, as well as one of the resonances located in the multiplet at 12.75 ppm, can be assigned to py protons. The lack of symmetry (C_s) in the molecule precludes an accurate assignment of the spectrum. However, the broad resonances at ~−41.8, −26.4, and −23.0 ppm can be assigned tentatively to the 6- (6′-) protons of the bpy ligands. The assignment is based on previous observations by Drago and DeSimone that for a series of bipyridyl complexes of Fe(III), Ru(III), and Os(III) the resonances are broader for protons which reside near the metal center because of proximal relaxation effects.[21]

Addition of a 20-fold excess of free pyridine to a solution of *cis*-$[Ru^{IV}(bpy)_2(py\text{-}d_5)(O)]^{2+}$ in CD_3CN or D_2O gave no sign of pyridine exchange within 1 h at 20 °C as evidenced by the failure of ***bound*** pyridine resonances to appear in the spectra. Our results demonstrate that the pyridyl group in the Ru(IV) oxo complex is substitutionally inert and that the coordination site is not normally available as a binding site in the oxidation chemistry of *cis*-$[Ru^{IV}(bpy)_2(py)(O)]^{2+}$.

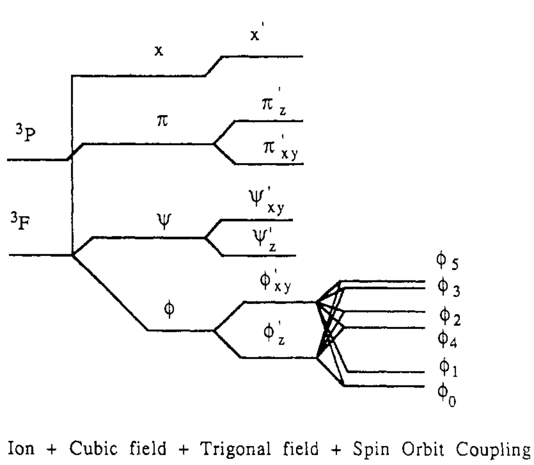

Figure 3. Energy level diagram for the d^4 Ru(IV) ion.[26]

In an effort to investigate further the nature of the contact shifts, the ^1H NMR spectrum of *cis*-$[Ru^{III}(bpy)_2(py)(OH)]^{2+}$ was recorded. Solutions of Ru(III) were prepared by mixing solutions containing equal concentrations of *cis*-$[Ru^{II}(bpy)_2(py)(OH_2)]^{2+}$ and *cis*-$[Ru^{IV}(bpy)_2(py)(O)]^{2+}$ in D_2O. A spectrum is shown in Figure 1C.

Solid-State Magnetic Measurements. The temperature variations of the magnetic susceptibility and magnetic moment for the salt *cis*-$[Ru^{IV}(bpy)_2(py)(O)](ClO_4)_2$ are shown in Figure 2. On the basis of the considerable paramagnetism, which approaches that expected for a $S = 1$ spin state at the room-temperature limit, several models were investigated in an attempt to reproduce the magnetic data on the basis of a $^3T_1$ ground state. Expressions developed by Kotani,[22] Griffith,[23] and Earnshaw et al.[24] are based on octahedral coordination around the central magnetic ion and are not expected to be fully adequate because of the low symmetry of the *cis*-$[Ru^{IV}(bpy)_2(py)(O)]^{2+}$ ion.

Low-symmetry models have been developed by Figgis et al.[25] and by Chakravarty,[26] with the latter having developed a closed-form expression for the case of a trigonal ligand field.[26] The 9-fold degeneracy of the $^3T_1$ term is lifted by spin–orbit coupling and by the low-symmetry crystal field component (Figure 3). The Hamiltonian can be written as

$$\hat{H} = \Delta(l - \hat{l}_z^{\,2}) - \alpha\xi\hat{l}_z\cdot\hat{s}_z - \alpha'\xi(\hat{l}_x\cdot\hat{s}_x + \hat{l}_y\cdot\hat{s}_y)$$

where Δ represents the energy difference between ϕ_z' (orbital singlet) and the ϕ_{xy}' (orbital doublet) in Figure 3. The constants α and α' are the parallel and perpendicular Lande factors, and ξ is the spin–orbit coupling constant. Solving the Hamiltonian matrix yields the corresponding eigenvalues and eigenstates. The solid line in Figure 2 is the best fit of the data to the relation in eq 6. In eq 6 *a*, *b*, *c*, and *d* are the coefficients for the corrected

$$\chi_{Ru} = \frac{8N\mu_B^{\,2}}{3k}\,\frac{(A^2/4T) + (2B^2k/D)(e^{D/kT} - 1)}{2 + e^{D/kT}} \tag{6}$$

$$A^2 = (2d^2 - c^2)^2$$

$$B^2 = \left(ac + bd - \frac{\alpha'}{\alpha}bc - \frac{\alpha'}{\alpha}ad\right)^2$$

$$D = {}^1\!/_2(S_0 - S_1 - \alpha\zeta)$$

$$S_0 = [(\Delta - \alpha\zeta)^2 + 8\alpha'\zeta^2]^{1/2}$$

$$S_1 = [\Delta^2 + 4\alpha'^2\zeta^2]^{1/2}$$

---

[21] DeSimone, R. E.; Drago, R. S. *J. Am. Chem. Soc.* **1970**, *92*, 2343.

[22] Kotani, M. *J. Phys. Soc. Jpn.* **1949**, *4*, 293.

[23] Griffith, J. *Trans. Faraday Soc.* **1958**, *54*, 1009.

[24] Earnshaw, A.; Figgis, B. N.; Lewis, J.; Peacock, R. D. *J. Chem. Soc.* **1961**, 3132.

[25] Figgis, B. N.; Lewis, J.; Mabbs, F. E.; Webb, G. A. *J. Chem. Soc. A* **1966**, 1411.

[26] Chakravarty, A. S. *Introduction to the Magnetic Properties of Solids*; Wiley: New York, 1981; pp 146–152.

Table II. Magnetic Parameters for *cis*-$[Ru^{IV}(bpy)_2(py)(O)](ClO_4)_2$

param	best fit value	param	best fit value
Δ	-1930 cm^{-1}	%I	0.98
ζ	872 cm^{-1}	g	2.0
α	0.907	A^2	4.820
α'	0.729	B^2	0.804

Table III. Temperature Dependence of the Chemical Shifts of Selected Peaks in the 400-MHz ^1H NMR Spectrum of *cis*-$[Ru^{IV}(bpy)_2(py)(O)](ClO_4)_2$ in CD_3CN

	chem shift, ppm (vs TMS)			
temp, K	py H[a]	bpy H		
235	62.8	66.8	−43.3	−58.0
245	60.6	64.3	−41.0	−54.8
255	58.4	61.8	−38.8	−51.8
265	56.3	59.5	−36.8	−48.8
275	54.4	57.4	−34.9	−46.2
285	52.5	55.4	−33.1	−43.8
295	51.0	53.7	−31.6	−41.5

[a] The assignment of the pyridine resonances is based on comparisons with the analogous perdeuterio derivative (Dobson, J. C. Ph.D. Dissertation, The University of North Carolina at Chapel Hill, Chapel Hill, NC, 1987).

wave functions. The line shown drawn through the temperature-dependent magnetic moment is related to the magnetic susceptibility expressed by $\mu_{eff} = 2.828(\chi_{Ru}T)^{1/2}$. A small impurity whose magnetic properties obscured the magnetic susceptibility below 4 K was incorporated into the model by assuming

$$\chi_{obs} = \chi_{Ru} + \chi_{impurity} \qquad (7)$$

If it is further assumed that an $S = {}^1/_2$ impurity is present as expected for a d^5 Ru(III) impurity and that it obeys the Curie law, the total magnetic susceptibility is given by eq 8. In eq 8

$$\chi_{total} = [\chi_{Ru}(1 - (\%I/100))] + [(Ng^2\beta^2S(S + 1)(\%I/100))/3kT] \qquad (8)$$

%I is the percent impurity. The g value was held constant at 2.0 in all of the calculations. The best fit parameters in Table II were obtained by using a simplex nonlinear least-squares program.[27,28] The minimum value of the function

$$F = \sum_i (\chi_i^{obsd} - \chi_i^{calcd})^2/(\chi_i^{obsd})^2$$

served as the best fit criterion. With the nonmagnetic state lying lowest, a doubly degenerate magnetic state lies at 79 cm^{-1} and all other states are calculated to be 1500–3000 cm^{-1} higher in energy.

The magnetic properties of the ion were also investigated in solution by measuring the temperature dependence of the chemical shifts in the ^1H NMR spectrum of *cis*-$[Ru^{IV}(bpy)_2(py)(O)](ClO_4)_2$. The results are summarized in Table III. Neglecting dipolar shifts, the chemical shift (δ_{obsd}) is given by McConnell's contact shift equation (eq 9).[29]

$$\delta_{obsd} = (K/T)\sum_i A_i\chi_i + \delta_{dia} \qquad (9)$$

In eq 9

$$K = \frac{|\gamma_e|}{3k_B|\gamma_H|} = 1.05 \times 10^{-8} \text{ kHz}^{-1}$$

and

$$\chi_i = \frac{n_i e^{\epsilon_i/kT}}{\sum n_i e^{\epsilon_i/kT}}$$

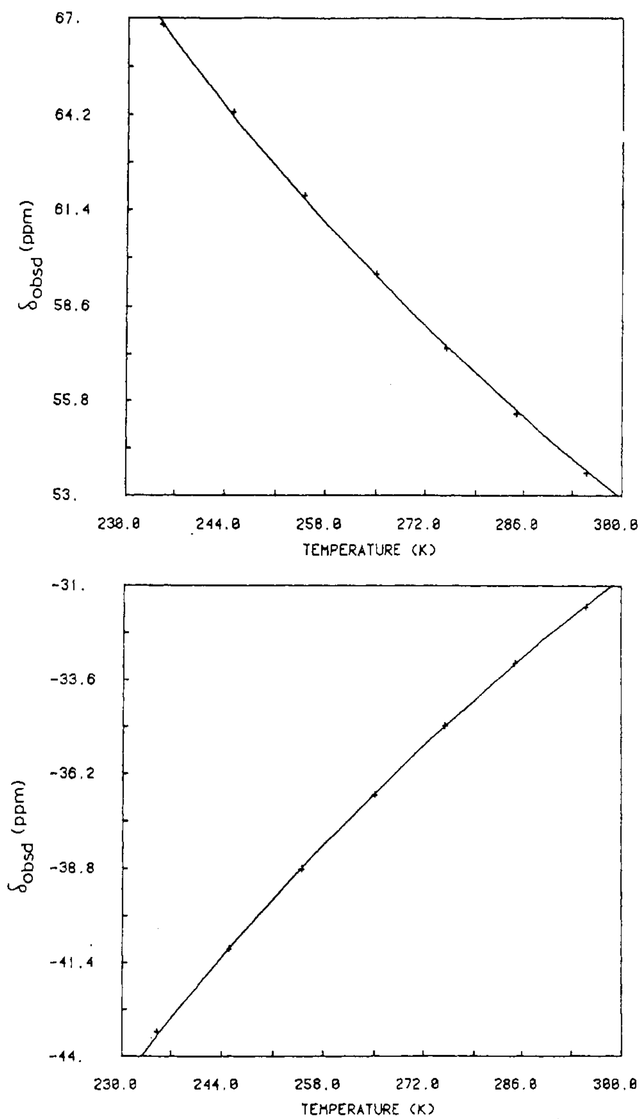

Figure 4. Temperature dependence of the chemical shift in the ^1H NMR spectrum for selected resonances of *cis*-$[Ru^{IV}(bpy)_2(py)(O)](ClO_4)_2$ in CD_3CN.

Table IV. Solution Magnetic Parameters for *cis*-$[Ru^{IV}(bpy)_2(py)(O)](ClO_4)_2$ in CD_3CN

param	best fit value[a]	param	best fit value[a]
Δ	-1195 cm^{-1}	A_1	11.02 MHz
ζ	936 cm^{-1}	A_2	-10.18 MHz
α	0.904	δ_1(dia)	8.98 ppm
α'	0.633	δ_2(dia)	9.01 ppm
		$E(\phi_1)$	56 cm^{-1}

[a] From the data presented in Figure 4.

The multiplicity factor n_i is $n_i = 2S_i + 1$. The summation is over all of the low-lying states that contribute to the ground-state electronic properties of the ion. A_i is the electron–nuclear hyperfine coupling constant, and the energy is $\epsilon_i = -J[S_i(S_i + 1)]$.

The fit of the data to the chemical shift equation adapted to the model described earlier but including contributions from only the two lowest states is shown in Figure 4 for two of the 2,2′-bipyridine resonances. The resulting best fit parameters are listed in Table IV. Discrepencies exist between the solution and solid-state values obtained for ζ, Δ, and the energy of ϕ_1 (56 vs 79 cm^{-1}). There may be real differences between the two, but the solution NMR data were acquired over the rather narrow temperature range of 70 °C and are less precise.

Discussion

The magnetic results obtained here are consistent with results obtained for other Ru(IV) oxo complexes. The structures of the cations *trans*-$[RuCl(O)(py)_4]^+$ and *trans*-$[Ru^{IV}(tmc)(MeCN)$-

---

(27) Oneil, R. *Appl. Stat.* **1971**, *20*, 338.
(28) Nelder, J. A.; Mead, R. *Comput. J.* **1965**, *7*, 308.
(29) McConnell, H. M.; Robertson, R. E. *J. Chem. Phys.* **1958**, *27*, 1361.

$(O)]^{2+}$ (tmc is 1,4,8,11-tetramethyl-1,4,8,11-tetraazacyclotetradecane) have been determined by X-ray crystallography.[2] In both cases the ions have been found to be paramagnetic at room temperatures with susceptibilities $\mu_{\mathrm{eff}} \approx 2.94\ \mu_B$, which are comparable to those found here.

The magnetic results are consistent with intuitive ligand field arguments.[30] For the d^4 ion the expected pattern of $d\pi$ levels is $d\pi_1 < d\pi_2$, $d\pi_3$. If the z axis is defined to lie along the Ru–oxo bond, the orbital ordering becomes $d_{xy} < d_{xz}$, d_{yz}. The splitting between d_{xy} and d_{xz}, d_{yz} is a consequence of $d\pi$–$2p_0$ mixing. It is that mixing and p_0 to $d\pi$ electronic donation that leads to the multiple-bonding character in the Ru–oxo interaction and to antibonding character in d_{xz}, d_{yz}. In the low symmetry of the complex, the d_{xz}, d_{yz} pair will be nondegenerate but the splitting between d_{xy} and d_{xz}, d_{yz} is expected to be much larger than the splitting between d_{xz} and d_{yz} because of the importance of the Ru(IV)–oxo interactions. The expected energy ordering scheme is $d\pi_1 \ll d\pi_2 < d\pi_3$, where the $d\pi$ orbitals are composed of appropriate linear combinations of d_{xy}, d_{xz}, and d_{yz}.

On the basis of the simple orbital arguments outlined above, the ground state for a d^4 ion is predicted to be either a magnetic singlet of electronic configuration $(d\pi_1)^2(d\pi_2)^2(d\pi_3)^0$ or a triplet of configuration $(d\pi_1)^2(d\pi_2)^1(d\pi_3)^1$. From the magnetic data, the singlet is lowest lying with the magnetic state lying slightly higher, at 79 cm^{-1} in the solid state and 56 cm^{-1} in CD_3CN.

The model[26] based on trigonal splitting of a ^3T state satisfactorily fits the data and is also consistent with the simple ligand field model. The values of the spin–orbit coupling constant, ζ, obtained from the fits are reasonable given the "free-ion" value of 1400 cm^{-1} for Ru(IV).[31] The negative value of Δ is consistent with a nonmagnetic "singlet" ground state.

Implications for Reactivity. In principle and in practice spin effects can play an important role in oxidation–reduction reactions. Two of the most prominent examples are the kinetically slow oxidations associated with molecular oxygen[31,32] and the contributions from spin effects to the nonadiabatic character of the $[Co(NH_3)_6]^{3+/2+}$ self-exchange reaction.[33-35] For example, for the latter case there is a change between high- and low-spin states between $[Co(NH_3)_6]^{2+}$ ($^4T_{1g}$–$t_{2g}{}^5e_g{}^2$) and $[Co(NH_3)_6]^{3+}$ ($^1A_{1g}$–$A_{2g}{}^6$). There are no spin coordinates in the electrostatic operator that induces electron transfer and, to zero order, no basis for electronic coupling between $[Co(NH_3)_6]^{2+}$ and $[Co(NH_3)_6]^{3+}$. However, the total spin inhibition to electron transfer is removed by including spin–orbit coupling. Spin–orbit coupling has the effect of mixing into the ground-state excited states of higher spin multiplicity, which creates a basis for electronic coupling between the $^4T_{1g}$ and $^1A_{1g}$ states of $[Co(NH_3)_6]^{2+}$ and $[Co(NH_3)_6]^{3+}$. In fact, for this case Zerner and co-workers have calculated that the energy of the ^2E excited state of $[Co(NH_3)_6]^{2+}$ at the metal–ligand distances appropriate to electron transfer is comparable to or even below that of $^4T_{1g}$. The electron-transfer mechanism may involve the conversion from $^4T_{1g}$ to ^2E followed by electron transfer from ^2E.[35] Electron transfer via the ^2E state is spin-allowed.

For second- and third-row transition-metal ions, spin–orbit coupling is large and extensive mixing between the ground and excited states of other multiplicities is possible. The possibility of significant spin effects still exists especially for complex mechanisms involving atom transfers where vibrationally induced electronic coupling must play a major role.

Spin effects could play a role, for example, if the d^4 ion were a triplet rather than a singlet ground state. For either case there is no spin prohibition in pathways involving H atom transfer. In the oxidation of H_2O_2, for example, spin can be conserved for either of the magnetic states as long as the Ru(III) + HO_2 redox products retain the triplet or singlet spin character of the reactants following the H atom transfer:

$$\begin{array}{llll}
\textit{cis}\text{-}[\mathrm{Ru^{IV}(bpy)_2(py)(O)}]^{2+} + \mathrm{HOOH} \rightarrow & & & \\
\quad (d\pi_1)^2(d\pi_2)^1(d\pi_3)^1 \qquad (\sigma_{O-O})^2 & & & \\
\quad (d\pi_1)^2(d\pi_2)^2(d\pi_3)^0 \qquad (\sigma_{O-O})^2 & & & \\
 & \textit{cis}\text{-}[\mathrm{Ru^{III}(bpy)_2(py)(OH)}]^{2+} + \mathrm{OOH} & & \\
 & \quad (d\pi_1)^2(d\pi_2)^2(d\pi_3)^1 \qquad (\sigma_{O-O})^1 & & \\
 & \quad (d\pi_1)^2(d\pi_2)^2(d\pi_3)^1 \qquad (\sigma_{O-O})^1 & &
\end{array}$$

For 2e transfer pathways involving hydride transfer to the oxo group (reaction 3) or O atom transfer from $Ru^{IV}{=}O^{2+}$ to the reductant, reactions 4 and 5, there is a spin inhibition to oxidation by a triplet oxidant. The spin prohibition exists because the products of reactions 4 and 5, Ru(II) + $OPPh_3$ or $ArCHOH^+$, are diamagnetic. Given the manifold of magnetic and nonmagnetic states for the ^3T configuration in Figure 3, mixing with low-lying nonmagnetic states will lift the total spin inhibition. However, if the lowest state of the oxidant remains largely triplet in character, the extent of vibrationally induced electronic coupling will be greatly diminished compared to that for a singlet state. As discussed in ref 5b, the extent of vibrational distortion required to achieve a surface crossing between reactants and products will be considerably larger than for a totally spin allowed reaction. The effect on the energy barrier to atom transfer could be large. For a $Ru^{IV}{=}O$ oxidant having a lowest lying triplet state, $E(\phi_1) < E(\phi_0)$ in Figure 3, a higher energy singlet state could play the same role in atom-transfer reactivity as the ^2E state of $[Co(NH_3)_6]^{2+}$ in $[Co(NH_3)_6]^{3+/2+}$ self-exchange.[35] For such a case, the expression for the rate constant would include a Boltzmann population term for the reactive singlet state of the form $[\exp(-E(\phi_0)/kT)]/[3 + \exp(-E(\phi_0)/kT)]$ as well as the barrier for atom transfer from the singlet state.

For *cis*-$[Ru^{IV}(bpy)_2(py)(O)]^{2+}$ as oxidant, there are no spin problems associated with oxidative reactivity. From the analysis of the magnetic data, the oxidant has a largely "singlet" ground state. There is a higher lying "triplet" state separated from the ground state by 79 cm^{-1} in the solid state and 56 cm^{-1} in solution. The energy spacing between the two states is sufficiently small that they are both significantly populated at room temperature, where $k_BT \approx 200\ cm^{-1}$. Interconversion between the states should be rapid. The narrow line widths in the contact-shifted ^1H NMR spectrum for the Ru(IV) oxo complex are consistent with rapid interconversion between intramolecular spin states with the "rapid exchange limit" being maintained down to −40 °C in CD_3CN.

Given the small energy gap and rapid interconversion between states, the $Ru^{IV}{=}O^{2+}$ ion has access to either spin state. More importantly, because of the singlet ground state there is no basis for a spin inhibition in 2e oxidation pathways.

Acknowledgment is made to the National Science Foundation under Grant No. CHE-8601604 for support of this research.

Registry No. *cis*-$[Ru^{IV}(bpy)_2(py)(O)](ClO_4)_2$, 120056-29-3.

---

(30) Nugent, W. A.; Mayer, T. J. *Metal-Ligand Multiple Bonds*; Wiley: New York, 1988; Chapter 2.

(31) Goodman, B. A.; Raynor, J. B. *Adv. Inorg. Chem. Radiochem.* **1970**, *13*, 192.

(32) Taube, H. *J. Gen. Physiol.* **1965**, *49*, 29.

(33) Hammershi, A.; Geselowitz, D. A.; Taube, H. *Inorg. Chem.* **1984**, *23*, 979.

(34) Buhks, E.; Bixon, M.; Jortner, J.; Navon, G. *Inorg. Chem.* **1979**, *18*, 2014.

(35) Larsson, S.; Stahl, K.; Zerner, M. C. *Inorg. Chem.* **1986**, *25*, 3033.